Food Chemistry: Molecular Sciences 5 (2022) 100137

Contents lists available at ScienceDirect

Food Chemistry: Molecular Sciences

journal homepage: www.sciencedirect.com/journal/food-chemistry-molecular-sciences

Unaided efficient transglutaminase cross-linking of whey proteins strongly impacts the formation and structure of protein alginate particles

Mikkel Madsen [a], Sanaullah Khan [a], Sonja Kunstmann [a], Finn L. Aachmann [b], Richard Ipsen [c], Peter Westh [a], Cecilia Emanuelsson [d], Birte Svensson [a,*]

[a] Department of Biotechnology and Biomedicine, Technical University of Denmark, DK-2800 Kgs. Lyngby, Denmark
[b] Norwegian Biopolymer Laboratory (NOBIPOL), Department of Biotechnology and Food Science, NTNU Norwegian University of Science and Technology, N-7491 Trondheim, Norway
[c] Department of Food Science, University of Copenhagen, DK-1958 Frederiksberg, Denmark
[d] Department of Biochemistry, Lund University, 223 62 Lund, Sweden

ARTICLE INFO

Keywords:
LC-MS/MS cross-link identification
Size exclusion chromatography
Dynamic light scattering
Far- and near-UV CD
Intrinsic and ANS fluorescence spectra
Molecular dynamics inter-residue distance analysis

ABSTRACT

There is a dogma within whey protein modification, which dictates the necessity of pretreatment to enzymatic cross-linking of β-lactoglobulin (β-Lg). Here microbial transglutaminase (MTG) cross-linked whey proteins and β-Lg effectively in 50 mM $NaHCO_3$, pH 8.5, without pretreatment. Cross-linked β-Lg spanned 18 to >240 kDa, where 6 of 9 glutamines reacted with 8 of 15 lysines. The initial isopeptide bond formation caused loss of β-Lg native structure with $t_{1/2} = 3$ h, while the polymerization occurred with $t_{1/2} = 10$ h. Further, cross-linking effects on protein carbohydrate interaction have been overlooked, leaving a gap in understanding of these complex food matrices. Complexation with alginate showed that β-Lg cross-linking decreased onset of particle formation, hydrodynamic diameter, stoichiometry (β-Lg/alginate) and dissociation constant. The complexation was favored at higher temperatures (40 °C), suggesting that hydrophobic interactions were important. Thus, β-Lg was cross-linked without pretreatment and the resulting polymers gave rise to altered complexation with alginate.

1. Introduction

Food science focuses on combining proteins with different properties, in homo- and hetero-polymeric complexes by cross-linking. Dairy and vegetable proteins were among the first subjected to cross-linking by transglutaminase. While caseins and pea 11S- and 7S globulins reacted easily, β-lactoglobulin (β-Lg) barely polymerized. Whey is an important food supplement and ingredient available in huge quantities from cheese-manufacturing. β-Lg is a safe, natural, well known food ingredient and has been shown to bind health-beneficial vitamins, hereby boosting its nutritional value (Mensi et al., 2013). Further, β-Lg has been shown to trigger or prevent allergenicity depending on ligand binding (Roth-Walter et al., 2021). β-Lg cross-linking is dogmatized to require pretreatment to occur. However, this dogma has arisen from a small experimental foundation. The various pretreatments used to facilitate microbial transglutaminase (MTG) cross-linking of β-Lg include, disulfide reduction by dithiothreitol (Tang & Ma, 2007), heating, strong alkaline conditioning, and proteolysis (Agyare & Damodaran, 2010; Partanen et al., 2011; Partschefeld et al., 2007). MTG is also used for biofabrication of functional soft matter by e.g. conjugating enzymes to gelatin (Liu et al., 2018). MTG reactive residues of β-Lg were probed by cross-linking with small reporter peptides and revealed cross-links at lysines 8, 77, and 141 and glutamines 35, 59, 68, and 155 (Nieuwenhuizen et al., 2004). Moreover, MTG-catalyzed incorporation of 5-(biotinamido)pentylamine preferentially occurred at glutamines 13, 68, either 115 or 120 and either 155 or 159 (Hemung et al., 2009). Thus, some β-Lg sidechains are clearly available for cross-linking by MTG, albeit they are shown to be with low reactivity (Eissa et al., 2006). In addition, chemical cross-linking by bifunctional reagents, e.g. disuccinimidyl suberate and the water-soluble bis(sulfosuccinimidyl)suberate (BS3) of about 11 Å in length form protein polymers by cross-linking of ε-amino groups (Seebacher et al., 2006).

Currently, only the direct impact of cross-linking on human health is studied, leaving out effects on the food matrix. Mixtures of whey proteins and alginate are widely applied in food and also pharma industries in emulsions, for texturizing and in microencapsulation of bioactive compounds or probiotic bacteria (Wichchukit et al., 2013). Alginate is a linear anionic polysaccharide extracted from seaweed, which consists of

* Corresponding author.
E-mail address: bis@bio.dtu.dk (B. Svensson).

https://doi.org/10.1016/j.fochms.2022.100137
Received 14 June 2022; Received in revised form 8 September 2022; Accepted 17 September 2022
Available online 19 September 2022

the 1,4-linked C-5 epimers β-D-mannuronate and α-L-guluronate, variably arranged in the polysaccharide (Schiener et al., 2015).

Protein cross-linking and hydrocolloid complexation both represent commonly applied approaches to modulate molecular interactions in the food matrix and manipulate food texture (Grossmann et al., 2017; Yousefi & Jafari, 2019). Here, a combination of these techniques is introduced using important food ingredients, alginate, β-Lg and whey protein. MTG is demonstrated to cross-link β-Lg, as well as a mixture of whey proteins, under mild alkaline conditions without heating or any other pretreatments. The most abundant β-Lg cross-link found was Q115-K14, followed by Q35-K14, Q115-K60, Q115-K70 and Q120-K75. Previously, interactions between alginate and β-Lg were shown to depend on electrostatic interactions (Gorji et al., 2018; Madsen et al., 2021; Stender et al., 2018). However, the cross-linked β-Lg and whey protein showed changes in surface chemistry such that alginate complexation involved hydrophobic interactions and the degree of protein polymerization influenced stoichiometry, affinity and particle size.

2. Materials and methods

2.1. Materials

2.1.1. β-Lactoglobulin and whey proteins

β-Lg A was purified from cow's milk by ultrafiltration and anion exchange chromatography, as previously described (Kristiansen et al., 1998) and stored in freeze dried form (−20 °C). Serum protein concentrate (SPC; generous gift by Jacob H. Nielsen; Arla Food Ingredients, Viby, Denmark) is a spray dried pilot scale production of concentrated whey proteins processed from milk (96.7% dry matter as 93.7% protein (81.7% β-Lg, 13.3% α-lactalbumin, 1.6% glycomacropeptide, 0.4% fat, 1.8% ash, 0.09% lactose and 0.025% calcium, according to the manufacturer, Arla Food Ingredients, Viby, Denmark). Prior to use, 10 mg/mL β-Lg or SPC was dissolved in double deionized water (dH_2O) overnight with gentle stirring (4 °C, 150 rpm), centrifuged (20,000 *g*, 20 min, 4 °C), filtered twice (0.22 μm syringe filter; Frisenette Aps, Denmark) and dialyzed against dH_2O (Spectrum™ Labs Spectra/Por, Waltham, MA, USA, 5 kDa MWCO, 3 × 100:1 (vol:vol), 4 h, 4 °C). Protein solutions were stored (4 °C) and used within 5 d after dialysis, but are stable for several months in buffer.

2.1.2. Microbial transglutaminase

The commonly industrially used and academically researched MTG from *Streptomyces mobareansis* (Mostafa, 2020; Tokai et al., 2020) (generous gift of Jeppe Tams; Novozymes, Bagsværd, Denmark) was stored at −20 °C and equilibrated to R.T. before use.

2.1.3. Alginate

Sodium alginate (AlgM, as named in (Madsen et al., 2021)) of M_n = 139 kDa, polydispersity = 1.9, F(M) = 0.65, F(G) = 0.35 and M/G ratio = 1.8 (generous gift of Trond Helgerud; DuPont Nutrition and Bioscience, Haugesund, Norway), was previously used for β-Lg complexation (Madsen et al., 2021). AlgM (3 mg/mL) was dissolved in dH_2O (1 h, 50 °C, 250 rpm), incubated overnight (4 °C, 250 rpm), dialyzed against dH_2O (3 × 100:1 (vol:vol), 4 h, R.T.) and filtered thrice (0.8 -> 0.45 -> 0.22 μm syringe filters; Frisenette Aps, Knebel, Denmark). AlgM concentration was determined by the phenol sulfuric acid method as previously reported (Stender et al., 2018).

2.2. Methods

2.2.1. Microbial transglutaminase reaction and chemical cross-linking

β-Lg or SPC was dialyzed (Spectra/Por, Spectrumlabs, 5 kDa MWCO, 3 × 100:1 (vol:vol), 4 h, 4 °C) against 50 mM $NaHCO_3$ pH 8.5, concentrated to 10–20 mg/mL (3 kDa MWCO; Amicon Ultra 15 centrifugal filter; Merck, Kenilworth, NJ, USA) and treated at specified concentrations by MTG (4.2 TGHU/mL) in 2 mL (37 °C, 300 rpm, 24 h). Samples were 10x diluted in the dialysis buffer and protein concentration (mg/mL) was measured spectrophotometrically at 280 nm (NanoDrop™ Lite, Thermo Scientific™, MA, USA). Extinction coefficients of 0.937 and 1.15 mg/(mL·cm) for β-Lg and SPC, respectively, as calculated by ProtParam (Gasteiger et al., 2005), were used to convert spectrophotometric measurements to concentrations.

β-Lg was dialyzed against 100 mM sodium phosphate pH 8.5 and concentrated to 20 mg/mL as above. Solid Bis(sulfosuccinimidyl)suberate (BS3) at 10x the molar concentration of β-Lg, was added to 1 mL 20 mg/mL β-Lg and incubated (30 min, at R.T.). The reaction was quenched by adding 1 M Tris-HCl pH 7.5 to a resulting 50 mM Tris-HCl.

2.2.2. SDS-PAGE

To evaluate the resulting sizes of the MTG and BS3 cross-linking reactions, protein samples (10–40 μg/mL, 30 μL) were supplied with 10 μL 4× reducing sample buffer, vortexed, centrifuged (10,000*g*, 1 min), heated (80 °C, 10 min), cooled (2 min), and centrifuged (10,000*g*, 1 min). The supernatants (0.45–0.9 μg protein) were subjected to SDS-PAGE (Mini-PROTEAN TGX gels, BIO-RAD, Hercules, CA, USA), using 15 μL low molecular weight ladder (Mark12™, Invitrogen, Waltham, MA, USA), run in Tris/glycine/SDS buffer (BIO-RAD, USA) at 300 V, 15 min, or stopped when the indicator color reached the gel bottom. Gels were stained (0.1% Coomassie brilliant blue, 0.4% copper sulfate, 10% acetic acid, 40% EtOH, 30 min with shaking), rinsed in dH_2O, destained (5% glycerol, 10% acetic acid, 25% EtOH, 1 h) and stored in dH_2O.

2.2.3. Size exclusion chromatography

To measure cross-linking efficiency and separate resulting products according to size, samples (1–2 mL) of MTG treated β-Lg or SPC were transferred to new Eppendorf tubes, centrifuged (20,000 *g*, 20 min, 4 °C), and the supernatants were analyzed by size exclusion chromatography (Hiload 16/600 Superdex 200 pg column, Merck, Darmstadt, DE) in 50 mM NH_4HCO_3 pH 8.5 at a flowrate of 1 mL/min, monitored spectrophotometrically at 280 nm using an Äkta Purifier 100 FPLC (GE, Boston, MA, USA). Individual protein-containing fractions of 4 mL were frozen at −80 °C for 16–24 h, lyophilized and stored at −20 °C.

2.2.4. Ammonia assay

Ammonia is a by-product of MTG cross-linking, which we took advantage of to follow the reaction by quantification, using a modified Berthelot colorimetric assay (Ammonia Colorimetric Assay Kit II, BioVision Inc., CA, USA), where indophenol formation depends on the ammonia concentration. Standards (0–10 nmol ammonia, made from the kit stock of 10 mM) and samples (diluted 1000× in reaction buffer to match the absorbance range of the standards) were mixed (96 well plate) with 80 μL kit reagent 1 and 40 μL kit reagent 2 to a final volume of 220 μL, incubated (30 min, 37 °C), and the absorbance measured at 670 nm (Epoch microplate reader, BioTek, VT, USA). Absorbance values of standards fitted to a linear curve were used to quantify ammonia released by the MTG reaction.

2.2.5. Mass spectrometry

To elicit information on which residues were cross-linked, mass spectrometry was employed.

2.2.5.1. Sample preparation. Protein bands of interest were cut from SDS-PAGE gels, chopped into 1x1x1 mm cubes, transferred to low DNA binding Eppendorf tubes, destained by 100 μL stain-remove buffer (50 mM NH_4HCO_3 pH 8.0, 50% acetonitrile (ACN)), and incubated (30 min, 1000 rpm, 25 °C). After a short spin, supernatants were removed and the procedure was repeated until the gel pieces were transparent. ACN (500 μL) was added to each sample, incubated (10 min, gentle mixing), centrifuged, and the supernatant was removed, followed by addition of 10 mM Tris(2-carboxyethyl)phosphine, 40 mM chloroacetamide (50

μL), incubated (30 min, 300 rpm, 25 °C), added ACN (500 μL) and incubated (10 min, gentle mixing). The tubes were centrifuged, supernatants discarded, and trypsin (13 ng/μL, 10 mM NH_4HCO_3, 10% ACN, 30–50 μL) was added to cover the gel pieces, left on ice (120 min), and transferred to a heat block (O/N, 37 °C).

2.2.5.2. Peptide extraction and purification. Samples were supplied with 50 μL liquid (5% formic acid, 50% ACN), incubated (10 min, 37 °C) and centrifuged. Supernatants were removed, stored in new tubes, and the treatment repeated. The combined supernatants were dried (60 °C, under vacuum) and peptides were purified either by C18 stage tipping or SCX fractionation. Samples were eluted from C18 stage tips with 2x 30 μL 40% ACN, 0.1% formic acid; SCX was eluted in three 60 μL steps by 75 mM, 150 mM and 300 mM ammonium acetate. Eluted peptides were dried (60 °C, under vacuum), dissolved in 2% ACN, 1% trifluoroacetic acid, iRT (index retention time) peptides and 0.5–1.0 μg sample peptides were subjected to LC-MS/MS.

2.2.5.3. LC-MS/MS analysis. Peptides extracted after in-gel digestion were analyzed by LC-MS/MS on a Q Exactive Hybrid Quadrupole-Orbitrap Mass Spectrometer (Thermo Scientific, San Jose, CA, USA) with pre–separation on an EASY-Spray column, 50 cm × 75 μm ID, PepMap RSLC C18, 2 μm ES803 mounted on an EASY-nLC 1000 Liquid Chromatography system (Thermo Scientific, San Jose, CA, USA). The separation was run as a 70 min gradient of solvents A (0.1% formic acid in dH_2O) and B (80% acetonitrile, 0.1% formic acid) at a constant flow of 250 nL/min, starting at 6% B, increasing to 23% over 43 min, followed by increasing to 38% over 12 min and completed by reaching 60% in 5 min. The column was finally washed with 95% solvent B for 10 min.

MS spectra were obtained in data-dependent acquisition mode with the following top 10 HCD method: Scan range was 300–1750 *m/z* and full scan resolution was 70,000 *m/z* with an AGC target of $3 \bullet 10^6$ and a maximum injection time of 20 ms. Normalized collision energy was set to 35 with a dynamic exclusion time at 30 s. Ions in charge state 1 and unassigned, were excluded. For the MS/MS resolution was set to 17,500 *m/z* with AGC target of $1 \bullet 10^6$ and a maximum injection time of 60 ms.

2.2.6. Data analysis

2.2.6.1. ProteoWizard. To prepare the data for analysis in MassAI, data were transformed from .RAW format to .mgf format, by ProteoWizard (Chambers et al., 2012). Here, a filter was applied that performs centroiding on all spectra, using the default settings; PickerType = a low-quality local maxima algorithm, signal-to-noise ratio = 1.0, minimum peak spacing = 0.1, ms levels = 1.

2.2.6.2. MassAI. Cross-linked peptides were identified using the software MassAI (version August 2019), freely downloaded from https://www.massai.dk/. This software is specialized in detection and identification of cross-linked peptides (Söderberg et al., 2018). Data files formatted in Mascot Generic Format (.mgf-files) were first filtered to retain the most intense peaks file, then files were merged and cross-links in β-Lg were identified using the following search settings: protein sequence: β-Lg A (for primary structure see Supplementary material); fragmentation mode: collision-induced dissociation, 10 ppm MS accuracy, 0.2 Da MS/MS accuracy, porcine trypsin as enzyme with 3 missed cleavages allowed; variable modifications: reduced cysteine (–SH), oxidized- and non-oxidized-carbamidomethyl (IAA), oxidized methionine (M-ox). For BS3 cross-linking, BS3-internal x-link (x-linker), BS3-H20 (x-linker) and BS3-H20 (*N*-term) were used, for MTG cross-linking was used -N for lysine and glutamine. Cross-linking of modified peptides was also allowed in the search. By manual validation of the MS/MS spectra, cross-links were filtered and accepted if the following criteria were fulfilled: score >10, no major peaks unexplained and multiple fragmentations on both donor and acceptor peptide. Thus, large portions of the results are excluded to avoid false positives.

2.2.7. Circular dichroism

Circular dichroism was used for investigation into secondary and tertiary structure changes. Samples were dissolved in 2.5 mM NH_4HCO_3 pH 8.5 for far-UV (0.03 mg/mL) and near-UV (2 mg/mL) CD. Spectra were recorded at 250–190 nm (far-UV) and 360–260 nm (near-UV) in a 1 mm quartz cuvette (50 nm/min, 0.5 nm bandwidth, 2 s response time, 25 °C; Jasco high throughput J-1500 Spectrophotometer, Jasco International Co, Sennincho Hachioji, Japan). Five scans were averaged and smoothed.

2.2.8. Dynamic light scattering

DLS was used to measure sizes of native proteins, cross-linked proteins and protein-alginate particles. Protein samples (1 mg/mL) in 50 mM KH_2PO_4 pH 3.0 were filtered twice (0.22 μm syringe filter; Frisenette Aps, Knebel, Denmark). Samples of protein AlgM complexes (1 mg/mL and 0.38 mg/mL, respectively) were diluted 20x with 50 mM KH_2PO_4 to achieve transparency and not filtered prior to analysis. The intensity weighted mean size (referred to as hydrodynamic diameter going forward) was determined using a ZetaSizer Nano ZS (Malvern Instruments, Worcestershire, UK) (Qi et al., 2004), equipped with a 4 mW He-Ne laser, operating at 632.8 nm. Scattering was measured at 173° for proteins, dual angle of 13° and 173° for complexes and results were computed by ZetaSizer software (version 7.13, Malvern Instruments, Worcestershire, UK). The software derives hydrodynamic diameter from cumulant analysis by the DLS autocorrelation function and an exponential fitting expression, taking both polydispersity and peak broadening into account. Analysis was performed with 20 runs per measurement for each sample. Samples were stable for the duration of the experiment (60 s), but would sediment if left >10 min.

2.2.9. Zeta potential measurement

For information on the surface charge of native and cross-linked protein, zeta potential was measured. Samples from dynamic light scattering were further used for measuring electrophoretic mobility (ZetaSizer Nano ZS with a universal dip cell; Malvern Instruments, Worcestershire, UK), using laser Doppler velocimetry technique. The rate of molecule movement is measured, expressed as electrophoretic mobility (μe, m/s) and number weighted zeta potential is calculated using the Henry equation:

$$\zeta = \frac{3\eta}{2\varepsilon F(\kappa\alpha)}\mu_e$$

where ζ(mV) = ζ-potential of particles, μ_e = electrophoretic mobility, η = viscosity and ε = solvent dielectric constant. F(κa) = Henry's function.

2.2.10. Isothermal titration calorimetry

Information on affinity, stoichiometry and binding energies was obtained by ITC, using a NanoITC2G (TA Instruments, DE, USA) equipped with a 250 μL injection syringe. β-Lg, SPC, cross-linked products thereof, and AlgM were dialyzed together against 50 mM KH_2PO_4 pH 3.0 (5 kDa MWCO, 3× 100:1 (vol:vol), 4 h, 150 rpm, 4 °C). Concentrations were thereafter adjusted with the dialysate to 27 μM (0.5 mg/mL) β-Lg, SPC or their cross-linked products, and 2–8 μM alginate. By 30 injections, alginate was titrated into protein (in the cell), the first of 3 μL followed by 29 of 6 μL. A blank titration of alginate into buffer was subtracted from all experiments to account for heat of dilution. Raw data were analyzed against a model assuming equivalent, independent binding sites, using the manufacturer's software (NanoAnalyze Data Analysis, version 3.8.0; TA instruments, USA), to obtain apparent values of stoichiometry (n), dissociation constant ($K_{d,app}$), and enthalpy (ΔH_{app}) for the complexation. The first titration point was excluded in the fitting process. Gibbs free energy (ΔG_{app}) and entropy (ΔS_{app}) are calculated from the relations $\Delta G_{app} = -R \bullet T \bullet \ln(K_{d,app})$ and $-T \cdot \Delta S_{app} =$

$\Delta G_{app} - \Delta H_{app}$, where T is temperature in Kelvin.

2.2.11. Optical measurements by Probe Drum

Interaction between protein and alginate was monitored by a multichannel unshielded spectrophotometer (Probe Drum, Probation Labs, Lund, Sweden) (Søndergaard et al., 2015) that measures fluorescence, absorbance and static light scattering during automatic titration with stirring. A 0.5 cm cuvette was filled with 800 μL 13 μM (0.25 mg/mL) β-Lg, SPC or their cross-linked products; the syringe was filled with 4 μM AlgM. The Probe Drum was set to titrate in steps of 6 μL AlgM, mix (100 s) and measure emission at 280 nm excitation, absorbance and static light scattering, all in a 300–700 nm window, after each of 30 titration points. The data were presented using the manufacturer's program (PD viewer, Probation Labs, Lund, Sweden).

2.2.12. Intrinsic fluorescence

Cross-linking dependent changes in tertiary structure were assessed by following the intrinsic fluorescence of proteins. Samples (20 mg/mL) in 50 mM NH_4HCO_3 pH 8.5, unless otherwise stated, were analyzed with excitation at 280 nm, emission measurement at 320–380 nm and 250 rpm stirring at 37 °C (Jasco 8500 spectrophotometer; Jasco International Co, Sennincho Hachioji, Japan). Excitation and emission bandwidths were 5 nm with a response time of 0.5 s. Five spectra were measured and averaged to produce the resulting curves. Time resolved samples were automatically measured every hour with settings mentioned above.

2.2.13. Statistical analysis

AlgM, SPC and β-Lg are all one batch products to eliminate batch variation effects. All experiments were repeated thrice; means, standard

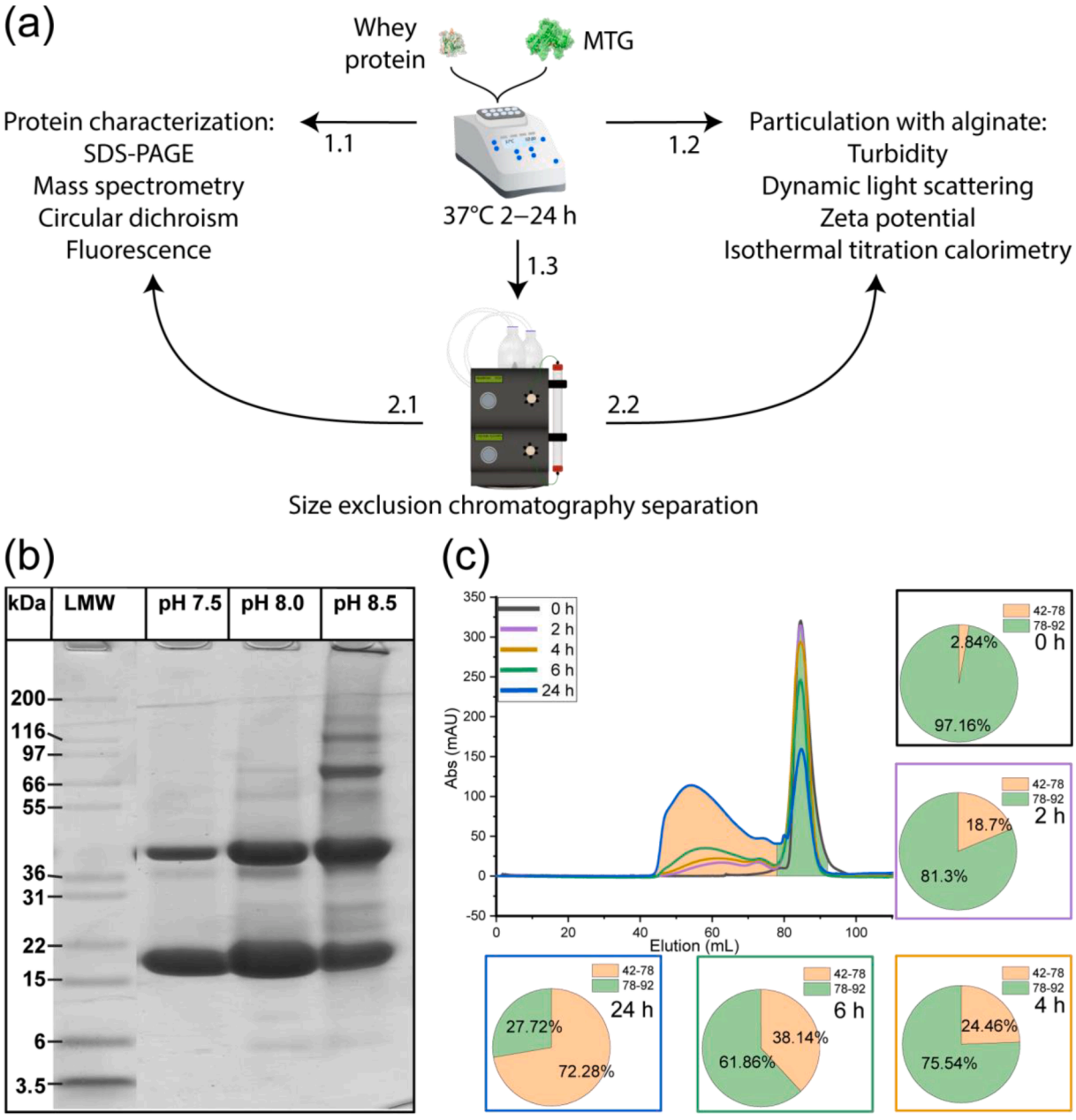

Fig. 1. pH-dependence of β-Lg cross-linking. (a) Methodological illustration of cross-linking and analysis. 1.1 and 2.1 are samples for protein characterization, 1.2 and 2.2 are samples for particulation with alginate and 1.3 is SEC analysis/separation. (b) SDS-PAGE of β-Lg (10 mg/mL) treated for 24 h with MTG (4.2 U/mL) at pH 7.5, 8.0, and 8.5. Left: low molecular weight marker. (c) SEC of β-Lg (20 mg/mL) reacted with MTG (4.2 U/mL) at pH 8.5 for 0 h (black), 2 h (magenta), 4 h (yellow), 6 h (green) and 24 h (blue). Pie diagrams represent the integrated areas: 42–79 mL (orange, polymerized) and 79–90 mL (light green, non-polymerized).

deviations and fits were calculated by OriginPro version 9.9.0.225.

3. Results

3.1. MTG cross-linking of β-Lg and SPC

The efficiency of MTG-catalyzed cross-linking of 10 mg/mL β-Lg at pH 7.5, 8.0 and 8.5, was evaluated by SDS-PAGE analysis after 24 h reaction (Fig. 1 (a)). Clearly, under these conditions, cross-linking of β-Lg beyond dimerization was only achieved at pH 8.5. Proceeding with cross-linking at pH 8.5, molecular sizes and yields of products after 2, 4, 6, and 24 h MTG-reaction of 20 mg/mL β-Lg were analyzed by size exclusion chromatography (SEC). This revealed increasingly polymerized β-Lg (Fig. 1 (b), purple, brown, green and blue lines, respectively) relative to untreated β-Lg monomer (Fig. 1 (b), black line) eluting at 85 mL. After 24 h polymers eluting at 44–78 mL corresponded to >70% of the total amount of β-Lg (Fig. 1 (b), blue line, Table S1). The $t_{1/2}$ of the polymerization was ~ 10 h as determined by plotting polymeric β-Lg (XL β-Lg) as a function of time and fitting to $\%XL\ \beta\text{-}Lg = \frac{\%XL\ \beta\text{-}Lg_{max} \cdot time}{t_{1/2} \cdot time}$ (Fig. S1 (a)). The $t_{1/2}$ for ammonia liberation in the MTG-reaction was also ~ 10 h (Fig. S1 (b)) and the ammonia released after 24 h corresponded to modification of about 80% of the glutamine residues in β-Lg. SDS-PAGE of SEC fractionated MTG-β-Lg reaction products confirmed abundant intermolecular covalent cross-linking (Fig. 2 (a)), covering a size range from >240 kDa (Lane 1, Fig. 2 (a)) to ~18 kDa of monomeric β-Lg (Lane 12, Fig. 2 (a)). DLS (Fig. S2) confirmed the formation of large β-Lg polymers with hydrodynamic diameter of 35 nm in SEC fraction 1 decreasing to 10 nm in fraction 11 (Fig. 1 (b), 2 (a) and S2). Polydispersity (Pdi) was found to be 0.1–0.3, thus the fractionated polymers were very homogenous. The optimized conditions for MTG reaction, similarly efficiently cross-linked 10 mg/mL SPC at pH 8.5 (Fig. S3). Notably, 55% of SPC was polymerized already after 6 h, as compared to 36% of 20 mg/mL β-Lg (Fig. 1 (a)), and 76% after 24 h (Fig. S4). MTG-treatment of 14 and 18 mg/mL SPC for 24 h, further increased polymer yields to 80% and 85%, respectively (Fig. S5).

3.2. Cross-links in β-Lg identified by LC-MS/MS and categorized by molecular dynamics-based measurement of inter-residue distances

To discover which residues were cross-linked by MTG during processing, samples from SDS-PAGE (Fig. 2 (a)) were excised and in-gel digested by trypsin for modified amino acid residue identification by LC-MS/MS. Altogether, forty cross-links distributed on 9 different glutamine-lysine pairs (Fig. 2 (b)) were found in peptides from the sampled lanes 1–9 (Fig. 2 (a)). The location of these reacting positions are illustrated on the structure of the β-Lg dimer (Fig. 3) assuming a certain spatial resemblance to the reacting form(s) of β-Lg (see also 3.3). Q115 and K14 appeared most frequently in cross-links, but no specific pair seemed to dominate and the cross-links Q35-K14, Q115-K60, Q115-K70 and Q120-K75 were equally abundant. These pairs, except Q115-K60, may be found in intermolecular cross-links, but as shown below (in 3.3) the early MTG-modifications appear to elicit conformational changes in β-Lg. Due to the low number of MS/MS peaks from the individual SDS band samples, the filtered mgf.-files were merged prior to cross-link identification to achieve reliable results, negating detection of cross-links based on the polymerization state of β-Lg. However, the evidence for efficient cross-linking was still robust.

A counterpart to enzymatic cross-linking is chemical cross-linking. Here, lysine residues in β-Lg were chemically cross-linked by BS3 as compared to the MTG-reaction. SEC showed distinct BS3 cross-linked β-Lg of sizes from 120 to 18 kDa in SDS-PAGE (Fig. S6 (a), (b)). Agreeing with residue surface exposure, 13 of the 15 lysine residues in β-Lg were represented in 37 identified cross-links (Fig. S7). Among the 13 different pairs, K8 and K75 reacted most frequently and appeared in 14 and 13 identified cross-links, respectively. K8-K135 and K75-K91 were the most common cross-links, each identified 8 times. Molecular dynamics distance measurement (Supplementary methods) was applied to help discern intermolecular and intramolecular cross-links (Fig. S8). Setting the distance cutoff for intermolecular cross-links to 20 Å based on the reported maximum distance BS3 is able to cross-link intramolecularly (Merkley et al., 2014), K83-K138 seemed an almost unique intermolecular bonds as the only other identified cross-link spanning >20 Å, K69-K100, was rare (Figs. S8, S9 and S10). The rest of the detected cross-links all matched the predicted minimum distance of <20 Å and may be intramolecular, although they cannot be excluded from including intermolecular cross-links.

3.3. Changes in β-Lg structure upon MTG cross-linking

The MTG cross-linked product was structurally analyzed, revealing processing alterations. SEC-fractionated MTG-treated β-Lg and SPC F1-F4 (F1 eluted at 44–48 mL, F2 at 52–56 mL, F3 at 60–64 or 72–76 mL and F4 at 80–88 mL, see Fig. S11), spanning four size ranges of decreasing degree of polymerization (DP), were each subjected to analyses of conformational features. Thus, far-UV CD spectroscopy indicated changes of secondary structure in β-Lg polymers shown by decreasing ellipticity at 204 nm for pools F1, F2, F3, as compared to

(a)

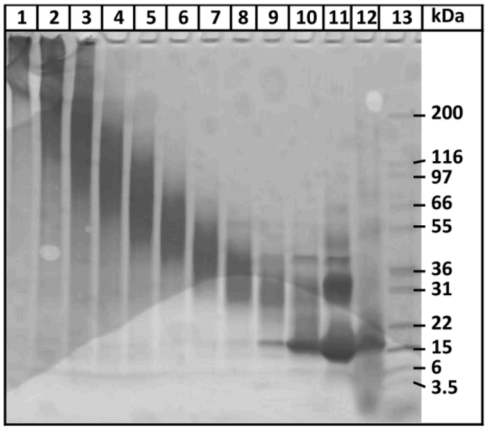

(b)

Count of result detections		Glutamine						Grand total
		5	13	35	59	115	120	
Lysine	14			6	3			9
	47					3		3
	60					7		7
	70					6		6
	75						6	6
	77	3						3
	91		3					3
	135	3						3
Grand total		6	3	6	3	16	6	40

Fig. 2. Polymerisation of β-Lg by MTG cross-linking. (a) SDS-PAGE after *SEC* of 2 mL 24 h cross-linked β-Lg (blue curve in Fig. 1). Lanes 1–12 (200 ng) each represent 4 mL fractions. Lane 13: low molecular weight marker. (b) Cross-links in polymeric β-Lg identified by LC-MS/MS. Numbers represent the times a cross-link was detected (gradient color-code: green, high; yellow, medium; red, few).

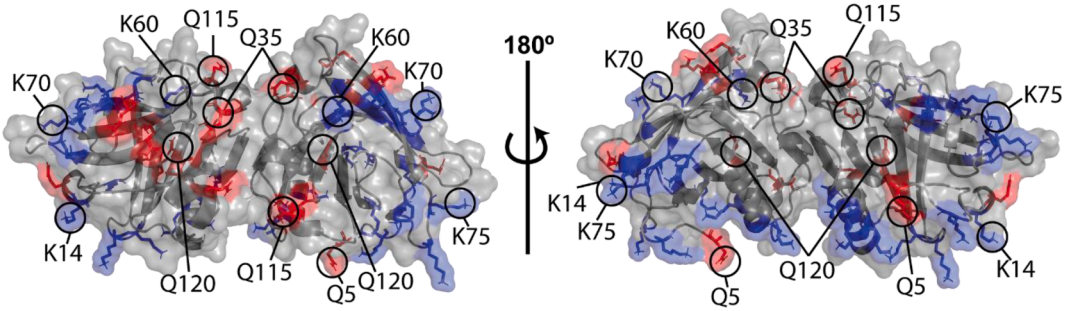

Fig. 3. Distribution of by MTG cross-linked amino acid residues on the β-Lg dimer (PDB: 1BEB)[1]. Glutamines (red) and lysines (blue). Highly cross-linked residues, as identified by LC-MS/MS, are numbered. Unreacted β-Lg surface (transparent grey), backbone (dark grey).

monomeric β-Lg in pool F4 (Fig. 4 (a) and S12). These ellipticity changes resembled those observed by heat-treatment of β-Lg (Fig. 4 (b)). Thus far-UV CD spectra were directly comparable to F4, F3, F2 and F1 and β-Lg heated at 30 °C, 70 °C, 75 °C and 80–90 °C, respectively (Fig. 4 (c)-(f)). Decreasing ellipticity at 295 nm of near-UV CD spectra also showed similarities between MTG-polymerized, respectively heat-treated β-Lg (Fig. S13). Far-UV CD spectra of β-Lg indicated a 20% reduction in secondary structure from pH 7.5 to 8.5 and a slight increase in T_m (Fig. S14 (f)), the decrease in secondary structure continued at pH 9.0 and only 10% remained at 9.5, as based on ellipticity values at 204 nm (Fig. S14).

During 0–24 h of MTG-treatment the intrinsic fluorescence of β-Lg gradually shifted maximum from 340 to 356 nm with a $t_{1/2}$ of 3 h (Fig. 5 (a), (b)). Continued monitoring of the MTG-reaction up to 60 h revealed a sudden increase in fluorescence intensity at 30 h (Fig. S15), implying that a new event occurred. This was not seen in a 60 h timespan for β-Lg in the absence of MTG (data not shown). The intrinsic fluorescence of β-Lg treated at 20–90 °C similarly shifted intensity maximum from 340 nm at 20 °C to 356 nm at 90 °C (Fig. S16). Finally, probing hydrophobic surface characteristics by 8-anilinonaphthalene-1-sulfonic acid (ANS) fluorescence, gave a signal at 480 nm, which increased both at higher concentration of untreated β-Lg (Fig. 5 (c), (d)) and with increasing DP of cross-linked β-Lg (Fig. 5 (d)). Notably, size-separated pools F1-F4 of 24 h MTG-cross-linked SPC gave only very small changes in intrinsic fluorescence at 320–400 nm (Fig. S17 (a)), far-UV CD (Fig. S17 (b)) and ANS fluorescence spectra (Fig. S17 (c)) in spite of the efficient cross-linking, emphasizing SPC being highly compatible with this food ingredient modification.

3.4. Interaction of alginate with cross-linked β-Lg and SPC

The hydrodynamic diameter of MTG-reacted β-Lg pools F1, F2, F3 and F4 was determined by DLS to 33, 16, 10 and 5 nm, respectively (Fig. 6 (a)), while it varied from 64 to 9 nm of SPC pools F1, F2, F3 and F4 (Fig. 6 (a)). The zeta-potential at pH 3.0 for β-Lg pools F1 through F4 slightly increased from 12 to 15 mV, conceivably reflecting the modification of ε-amino groups (Fig. 6 (b)). At pH 3.0, maximum turbidity at 600 nm was reached with 0.22 and 0.26 μM AlgM for F1 and F2 of cross-linked β-Lg, as opposed to 0.42 μM AlgM for both F3 and F4 (Fig. 6 (c)). Remarkably, hydrodynamic diameter analysis by DLS of MTG-treated either β-Lg or SPC complexed with AlgM showed particles of increasing size with decreasing DP for β-Lg or SPC polymers (Fig. 6 (d), Table S1; data for SPC not shown). Size distributions were wide for all particle measurements, with Pdi's >0.5.

ITC results of AlgM interaction with β-Lg, MTG-treated β-Lg (Fig. 6 (e)) and size fractionated β-Lg pools F1-F4 (Fig. 6 (f)), indicated that the DP affected stoichiometry (n), apparent dissociation constant ($K_{d,app}$) and enthalpy (ΔH_{app}) (Table S2). For pools F1-F4, $K_{d,app}$ decreased from 1.3 μM for F1 to 53 nM for F4, n (number of β-Lg molecules per AlgM molecule) decreased from 48 for F1 to 37 for F4, and ΔH_{app} increased from −15 for F4 to −11 kJ/mol for F1 and F2. The standard Gibbs free energy (ΔG°_{app}) increased from −42 for F4 to −34 kJ/mol for F1 and entropy (ΔS_{app}) from 72 to 87 J/mol for F1 through F4 as calculated from $K_{d,app}$ and ΔH_{app}. AlgM binding of the cross-linked SPC pools F1-F4 showed the same tendencies for $K_{d,app}$ and n (Fig. S18, Table S2).

To better understand the difference in interaction of alginate-β-Lg and alginate-(MTG treated β-Lg), the enthalpic and entropic contributions were examined. ΔH_{app} decreased with increasing temperature (Fig. S19 (a)). By applying a linear fit to ΔH_{app} as a function of temperature, a change of -239 ± 6 J/(mol•K) ($R^2 = 0.98$) was found, suggesting hydrophobic surface interaction between AlgM and cross-linked β-Lg (Schönbeck et al., 2014). Further, ΔS_{app} decreased from 32 J/(mol•K) at 5 °C to 3 J/(mol•K) at 40 °C (Fig. S19 (b)), also in accordance with hydrophobic interactions.

4. Discussion

4.1. Enzymatic cross-linking of β-Lg and SPC

Previously, cross-linking of whey proteins catalyzed by MTG at pH 7.0–8.0 showed that polymerization of β-Lg depends on unfolding of β-Lg by using different pretreatments or on mixing it with other whey proteins (Færgemand et al., 1997; Hemung et al., 2009; Nieuwenhuizen et al., 2004). As the MTG reaction mechanism involves unprotonated ε-amino groups (Miwa, 2020), we raised pH to 8.5 to advance β-Lg cross-linking. Further pH increase was not investigated as MTG unfolds at pH 9 (Ando et al., 1989) and in fact precipitated when diluted with 50 mM $NaHCO_3$ pH 9.0. Moreover, the activity of MTG is reduced at pH >8. Thus, as seen from the SDS-PAGE analysis, pH 8.5 was optimal for MTG cross-linking of β-Lg without pre-treatment. According to the manufacturer, the SEC resolves globular proteins up to 600 kDa. However separation in the 400–600 kDa range was poor, and cross-linked product eluting in the void volume (44 mL) was not resolved. Upon cross-linking, protein density and shape have been shown to change (Abbate et al., 2019). Thus, the molecular weight standards used in SEC with spectrophotometric detection do not directly indicate molecular weight of cross-linked products not behaving like Stokes-Einstein spheres. As reported SEC-MALS or gel electrophoresis can be used to get more accurate values (Raak et al., 2018). Reducing SDS-PAGE indicated cross-linked β-Lg ranging from dimeric (~38 kDa) to larger than dodecameric (>240 kDa, which is the size cutoff of the SDS-PAGE stated by the manufacturer). The same trend was observed for cross-linked SPC complexes that contained β-Lg as main constituent. As cross-linked products of molecular weight similar to that of dimeric β-Lg (determined by SDS-PAGE) eluted 12 mL earlier than native β-Lg dimer, it is suggested that cross-linking led to less compact protein structures. This however, requires additional analysis such as by SEC-MALS for confirmation. A study found that MTG treatment of gelated β-Lg (40 mg/mL, 85 °C for 20 min prior to cross-linking) had little effect, only preventing gel swelling (Murphy et al., 2017). In comparison, here MTG with great effect altered β-Lg prior to any functionalization, possibly enabling the formation of new gelation networks of different textures.

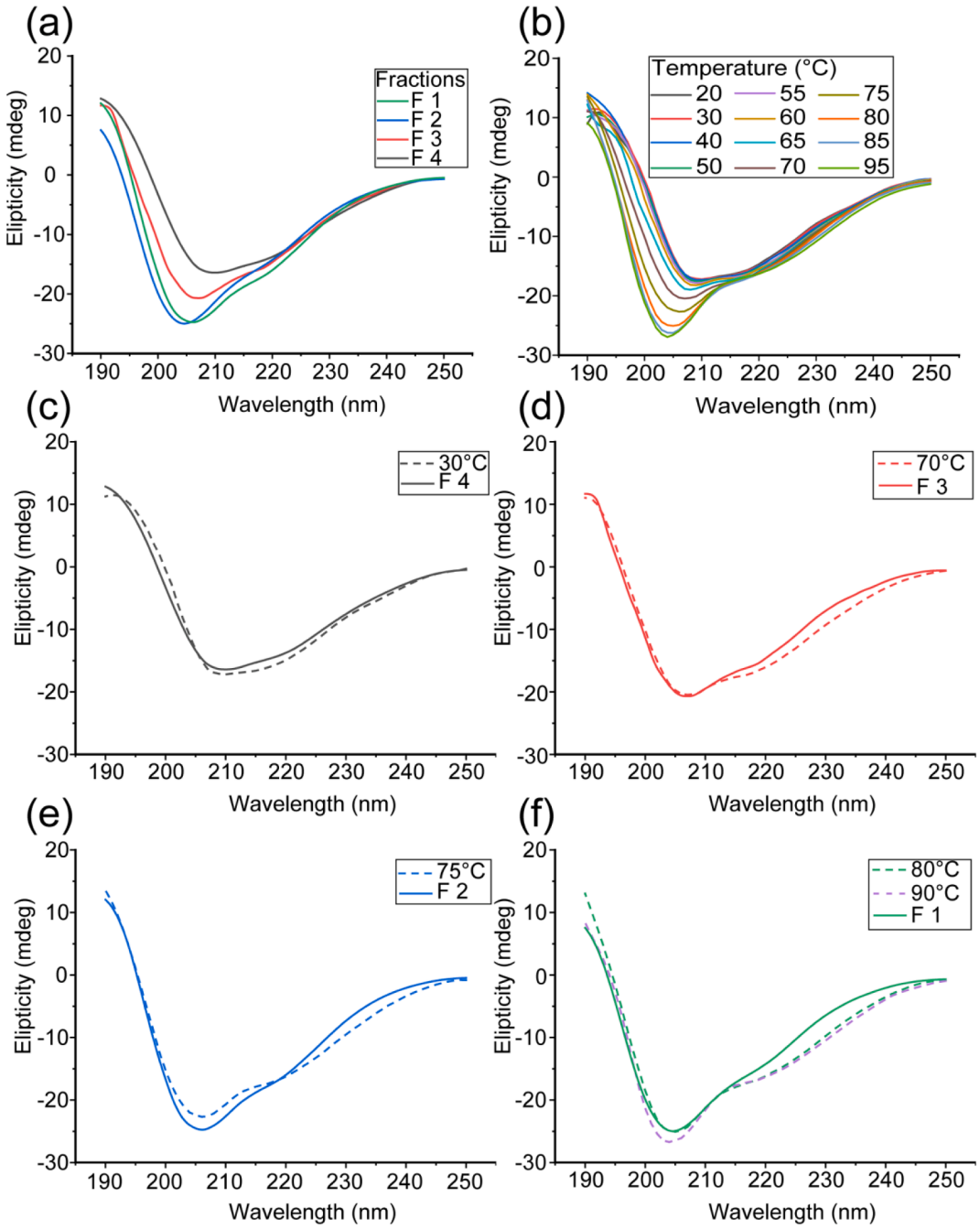

Fig. 4. Comparison of secondary structure changes in β-Lg after cross-linking and heat denaturation by Far-UV CD spectra at 250–190 nm. (a) F1 (green), F2 (blue), F3 (red) and F4 (black). (b) β-Lg in the range 20–95 °C. (c) F4 and β-Lg at 30 °C. (d) F3 and β-Lg at 70 °C. (e) F2 and β-Lg at 75 °C. (f) F1, β-Lg at 80 °C (green) and 90 °C (purple). Fractions are solid and temperatures are dashed lines.

Integration of SEC profiles for different MTG-reaction times, resulted in $t_{1/2} = \sim 10$ h of β-Lg cross-linking which reached >70% yield after 24 h in agreement with release of 80% of the predicted maximum amount of ammonia, corresponding to 7 molecules of ammonia per β-Lg or 7 formed cross-links (not taking eventual deamidation into account). Because β-Lg unfolds spontaneously at pH >9.0 (Taulier & Chalikian, 2001), the stability under the cross-linking conditions at pH 8.5 was debatable, but notably β-Lg neither polymerized nor underwent intrinsic spontaneous structural changes in the absence of MTG during 60 h. Thus, the cross-linking conditions did not elicit polymerization of β-Lg, as opposed to the previously reported cross-linking of β-Lg involving pre-treatment by heating and denaturation at alkaline pH (Eissa et al., 2006; Stender, Koutina, et al., 2018).

Chemical cross-linking by BS3 led to a series of β-Lg products of DP from two to seven as detected by SDS-PAGE and SEC (Fig. S6). Cross-links identified by LC-MS/MS reflected distinct reaction patterns compared to the MTG-reaction (Fig. 2 (b) and S7). BS3 thus modified 13 and MTG 7 of the 15 lysines in β-Lg. All 15 lysines are surface exposed and even K60, which is situated in a groove, reacted readily. Adopting the three-dimensional structure of β-Lg, intermolecular cross-links were anticipated based on lysine-lysine and lysine-glutamine inter-residue distances by aid of molecular dynamics (MD) (Fig. S8). Intramolecularly cross-linking by BS3 was considered for lysine residues of C^{α}-C^{α} distances up to 30 Å (Merkley et al., 2014), while here the cut-off distance was estimated by MD considering flexibility effects to <20 Å between nitrogens in lysine ε-amino groups. By accepting this constraint, only

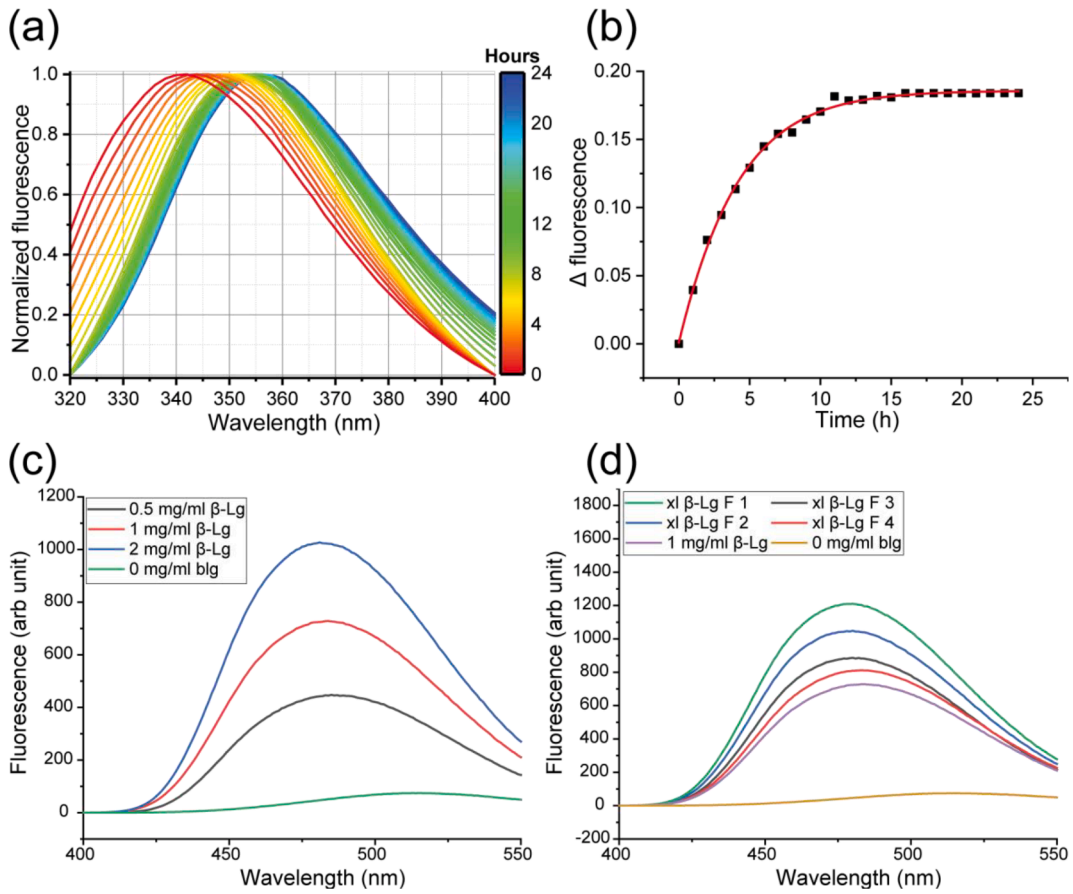

Fig. 5. Surface changes in β-Lg measured by fluorescence. (a) Fluorescence spectra during cross-linking reaction at 320–400 nm monitored with 1 h intervals (0–24 h) at pH 8.5. (b) Change in fluorescence intensity at 356 nm (from (a)). (c) ANS fluorescence of β-Lg 400–550 nm 0–2 mg/mL β-Lg. (d) ANS fluorescence of MTG cross-linked β-Lg pools F1-F4 (1 mg/mL) at 400–550 nm.

two intermolecular cross-links, K69-K100 and K83-K138, were identified for BS3, although it cannot be excluded that MS-identified cross-linked residues at shorter computed distances can belong to different β-Lg molecules. The chemical cross-linking pattern was found to be similar to that of the DMSO or DMF soluble cross-linkers DSS, DSG and BDRG (Seebacher et al., 2006). This gave evidence to a priority tendency of chemical cross-linkers to β-Lg. For MTG catalyzed cross-linking, it is not possible to set a distance limit, but minimum glutamine to lysine distances varied from 6.3 to 25.5 Å (Fig. S8). Restricted spatial access to the MTG active site is expected to play an important role in the apparent side chain reactivity (Miwa, 2020).

In β-Lg, 7 of the 9 glutamines are surface exposed and 6 were cross-linked by MTG (Fig. 2 (b)). Q115, reacting most frequently, was identified in 16 cross-links, and together with Q35 it is located in flexible loops at the mouth of the calyx of β-Lg (Fig. 3). The loop containing Q115 is affected by the Tanford transition, yielding a more open conformation of β-Lg above pH 7.5. This transition, does however not change the overall structure of β-Lg. Surprisingly, the hydrophobically buried Q120 was cross-linked. As MTG normally only reacts with exposed amino acid residues, the modification of Q120 spurred our investigation of the conformational integrity of the polymerized β-Lg.

4.2. *The conformation of β-Lg changes during MTG cross-linking*

Cross-linked products of β-Lg of increasing DP shifted the far-UV CD ellipticity minimum towards 204 nm (Fig. 4 (a)), reminiscent of denaturation of β-Lg by a temperature increase from 20 to 95 °C of 1 °C/min (Fig. 4 (b)). This corresponds to observations made by others, where heated β-Lg showed similarities to cross-linked β-Lg, most likely due to the formation of disulfide bridge networks in heated β-Lg (Krämer et al., 2017). Thus, MTG-polymerization of β-Lg and heat denaturation invoked similar loss of secondary structure. The far-UV CD spectrum of F4, which has the molecular size of native β-Lg, matched β-Lg at 30 °C, while that of F3, containing β-Lg of DP 4, aligned with β-Lg at 70 °C. Plotting normalized ellipticity at 204 nm for heat-treated β-Lg, revealed that only half of the β-Lg population was folded at 70 °C (Fig. S12). Normalization of CD spectra for pools F1-F4 showed that F4 is almost 100% folded, while F3 is 50%, F2 < 20% and F1 < 15% folded β-Lg. Differences in near-UV CD spectra of F1-F4 (Fig. S14), suggested changes in the tertiary structure and partial loss of native conformational integrity, which we conclude seemed to be crucial for the successful cross-linking of β-Lg by MTG.

During the MTG-reaction, the intrinsic fluorescence maximum shifted indicating a conformational change of β-Lg with $t_{1/2}$ = 3 h (Fig. 5 (a)), resembling the shift occurring by heat denaturation (Fig. S16). As this structural perturbation was faster than the polymerization ($t_{1/2}$ = 10 h), β–Lg loses some secondary structure at the beginning of the MTG treatment. It seemed that this 20% decrease in folding propensity (Fig. S14), thus not a complete unfolding, efficiently promoted the MTG-cross-linking at 37 °C. Around a reaction time of 30 h the intrinsic fluorescence underwent an immense increase. As β-Lg has only two tryptophans, one of which is reported to be quenched by water (Albani et al., 2014), this increase may indicate a structural rearrangement enabling both tryptophans to contribute a fluorescence signal when β-Lg is highly polymerized. Additionally, the fluorescence at 480 nm of ANS that probes changes in hydrophobicity (Collini et al., 2000) gradually increased for cross-linked β-Lg with higher DP, suggesting a quadrupling of the hydrophobic surface area (Fig. 5 (c), (d)).

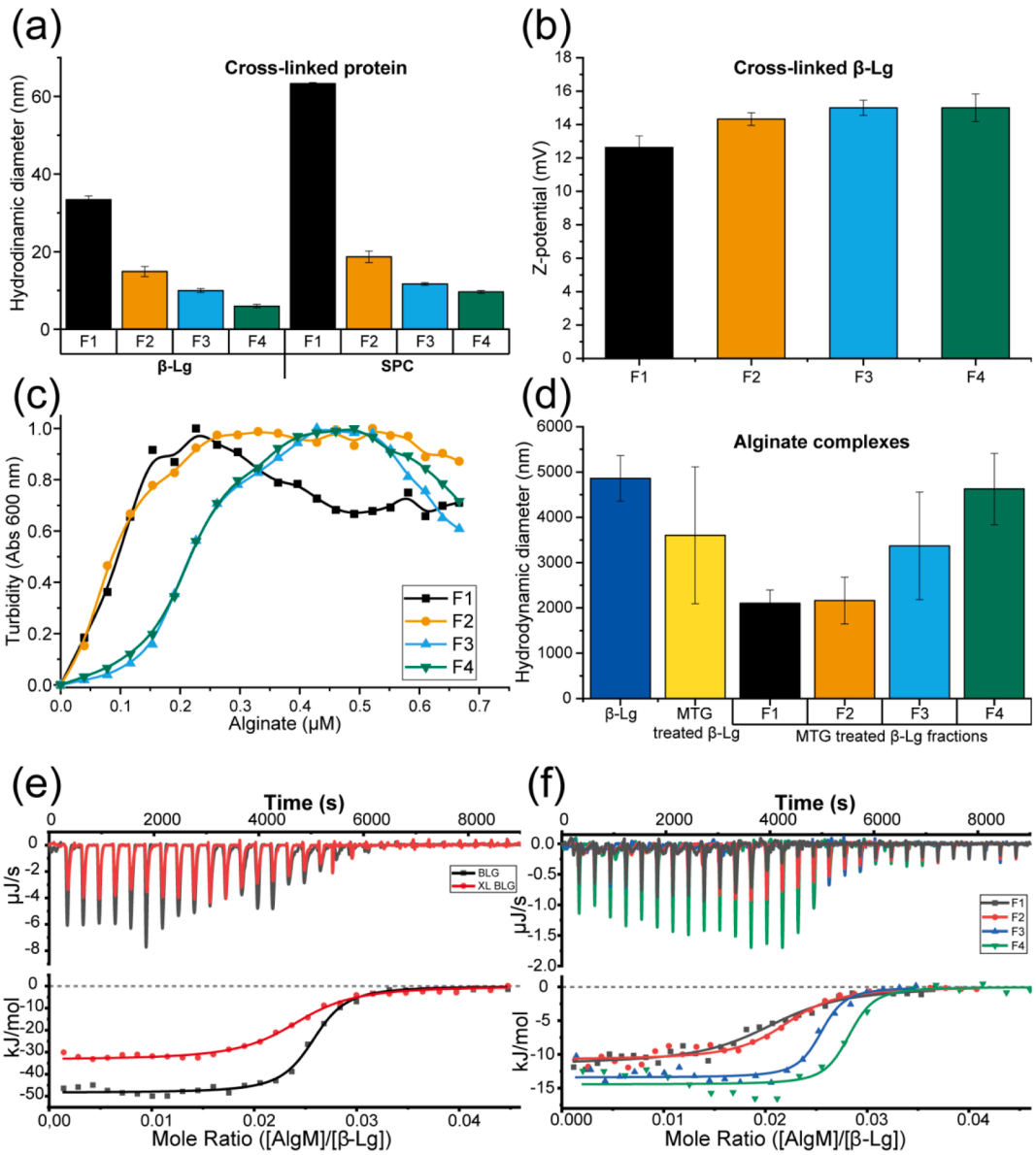

Fig. 6. Size and alginate binding of MTG cross-linked β-Lg. (a) Hydrodynamic diameter measured by DLS for β-Lg pools F1-F4 and SPC pools F1-F4. (b) Zeta-potential of β-Lg pools F1-F4. (c) Turbidity of β-Lg pools F1-F4 added AlgM. (d) Hydrodynamic diameter of β-Lg, MTG cross-linked β-Lg and pools F1-F4 in complex with alginate. F1 black, F2 orange, F3 light blue, F4 green, β-Lg blue and MTG treated β-Lg yellow. (e)-(f) ITC raw data (top) of β-Lg, MTG treated β-Lg (24 h) before and after *sEC*-fractionation, titrated with AlgM and enthalpograms with model fits (bottom). (e) β-Lg (black) and MTG treated β-Lg (red). (f) F1 (red), F2 (blue), F3 (black) and F4 (green).

A whey protein mixture has previously been shown to be readily cross-linked at pH 7.0 (Agyare & Damodaran, 2010), this was also the case for SPC (data not shown). At pH 8.5, SPC was >70% cross-linked, without any pretreatment or special reaction conditions. Intrinsic fluorescence, far-UV CD and ANS analyses all indicated lack of significant structural change in size-fractionated MTG-treated SPC pools F1-F4 (Fig. S17). Whey proteins not identified here and eluting earlier than β-Lg and α-lactalbumin in SEC of untreated SPC, may hold the key to why SPC was easily cross-linked compared to β-Lg. SDS-PAGE confirmed that the untreated SPC eluted in SEC from 44 to 76 mL as protein ensembles containing β-Lg, α-lactalbumin, lactoferrin, serum albumin and immunoglobulin (Fig. S20). Among these proteins, lactoferrin has been shown to form complexes with β-Lg, and may act as a chaperone that keeps β-Lg in its native state (Tavares et al., 2015).

4.3. Cross-linking of β-Lg and SPC changes the interaction with alginate

It is well known that complexation of positively charged proteins with the polyanionic alginate depends on electrostatic interactions (Madsen et al., 2021; Stender, Khan, et al., 2018). Alginate is also anionic at low pH (Klemmer et al., 2012) and β-Lg is positively charged below its pI of 4.8–5.2, which defines the suitable pH range for their interaction (Madsen et al., 2021; Stender, Khan, et al., 2018). In this light, SEC-fractionated pools F1-F4 of MTG-cross-linked β-Lg and SPC were adjusted to pH 3.0 before mixing with AlgM. DLS and zeta-potential analyses at pH 3.0, confirmed the hydrodynamic diameter of cross-linked pools (Fig. 6 (a)) to comply with those of cross-linked β-Lg at pH 8.5 (Fig. S2) and their positive net surface charge (Fig. 6 (b)). No major difference was indicated by DLS analysis of the protein samples between pH 8.5 and 3.0. CD spectroscopy also indicated no change in secondary structure to occur (data not shown), but we cannot exclude that more subtle conformational variation, such as changes in non-

folded regions, distinguishes cross-linked samples at these two pH values.

The maximum turbidity at 600 nm was reached by addition of AlgM at lower concentration for cross-linked β-Lg pools F1-F4 of higher DP (Fig. 6 (c)). Deeper insight into the impact of the polymerization was obtained by ITC (Fig. 6 (e), (f), Table S1), showing that $K_{d,app}$, stoichiometry (n) and ΔH_{app} all varied with the DP of cross-linked β-Lg. Native β-Lg carries a positive net charge at pH 3.0, but upon unfolding the charge density decreases, reflected by the 60-fold increase of $K_{d,app}$ from 53 nM to 1.3 μM. Alginate β-Lg complexation has been categorized as a surface interaction (Gorji et al., 2018; Madsen et al., 2021; Stender, Khan, et al., 2018) and probably the MTG-cross-linking at pH 8.5, raised the number of β-Lg molecules bound to AlgM from 35 to 43. The increase in ΔH_{app}, associated with polymerization is accompanied by a less pronounced increase in ΔG°_{app}, and a sharp increase in ΔS_{app}, reflecting a change in interaction mechanism compared to native β-Lg. The enthalpy and entropy changes correlated inversely with temperature changes, reflecting that the change in mode-of-interaction stemmed from increased surface hydrophobicity of cross-linked β-Lg (Schönbeck et al., 2014). Hydrophobic interaction was not previously reported for alginate β-Lg complexation or complexation of alginate with other proteins. However, in alginate, the uronate ring side opposite of the carboxylic acid is hydrophobic, and one study showed alginate and a cationic antimicrobial peptide (CDP – cysteine dense peptide – of 19 amino acids) interacting via hydrophobic bonds, inducing an α-helical conformation of the peptide (Kuo et al., 2007). As CDPs are intrinsically disordered and highly flexible, they adopt different conformations suiting the physicochemical environment. Because cross-linked β-Lg does not possess a thermodynamically favorable tertiary fold, its peptide backbone may be free to adopt conformations, allowing hydrophobic interactions with alginate, which are not possible for the native state of β-Lg. Notably, the estimated hydrodynamic diameter of AlgM complexes decreased with increasing DP of β-Lg in accordance with a certain compactness enforced by the cross-linking (Table S1). In general, alginate β-Lg complexation is driven by charge neutralization, which reduced the self-molecular charge repulsion of alginate. This charge neutralization pattern was altered by cross-linking of β-Lg, resulting in smaller complexes. Thus, MTG-polymerization affects both β-Lg and β-Lg alginate complexes. Similar, albeit less pronounced effects occurred for the SPC (Fig. S18).

5. Conclusion

It was found that >70% of β-Lg was cross-linked by MTG at pH 8.5 without any pre-treatment. Cross-links were formed between both surface exposed (Q35, Q115, K14, K60, K70 and K75) and core residing (Q120) side chains, and associated with partial loss of secondary and tertiary structure. By contrast, chemical cross-linking using BS3 did not alter the secondary structure of β-Lg, probably the flexibility and length of the linker ensured non-denaturing cross-linking. MTG cross-linking more efficiently formed larger polymers from a whey protein mixture (SPC), which has β-Lg as main component, with no evidence of loss of conformational integrity. This suggests, that MTG generated heteropolymeric protein complexes of β-Lg with other whey proteins, behave differently from homo-polymeric complexes of β-Lg, by protecting β-Lg from unfolding. The degree of polymerization strongly influenced the binding of alginate as established by changes in $K_{d,app}$, stoichiometry, enthalpy and hydrodynamic diameter. Temperature dependent enthalpic/entropic contribution suggests a hydrophobic driven mode-of-interaction of cross-linked β-Lg and alginate, not reported before. Thus, MTG-cross-linking of β-Lg or whey protein mixtures prior to interaction with alginate can lead to new functionalities, in the form of large networks and changes in complexation mechanism for application in the food industry.

CRediT authorship contribution statement

Mikkel Madsen: Conceptualization, Methodology, Software, Validation, Formal analysis, Investigation, Data curation, Writing – original draft, Writing – review & editing, Visualization, Project administration. **Sanaullah Khan:** Investigation, Writing – review & editing. **Sonja Kunstmann:** Methodology, Writing – review & editing. **Finn L. Aachmann:** Writing – review & editing. **Richard Ipsen:** Writing – review & editing. **Peter Westh:** Methodology, Validation, Writing – review & editing. **Cecilia Emanuelsson:** Methodology, Validation, Writing – review & editing. **Birte Svensson:** Conceptualization, Methodology, Validation, Resources, Writing – original draft, Writing – review & editing, Supervision, Project administration, Funding acquisition.

Declaration of Competing Interest

The authors declare that they have no known competing financial interests or personal relationships that could have appeared to influence the work reported in this paper.

Data availability

Data will be made available on request.

Acknowledgements

Karina Jansen (DTU Bioengineering) is gratefully acknowledged for technical support and Assist. Prof. Gael Clergeaud Veiga (DTU Health Tech) for DLS analyses. Science manager Jeppe W. Tams (Novozymes) is thanked for the MTG, seaweed R&D Leader Trond Helgerud (DuPont Nutrition and Bioscience) for AlgM, and Senior Innovation Manager Jacob Holm Nielsen (Arla Foods Ingredients) for SPC. We thank Prof. Jens Preben Morth for use of the fluorimeter and circular dichroism spectrometer and Prof. Alexander Büll and Dr. Emil G.P. Stender for introduction and use of ProbeDrum. All mass spectrometry was performed at DTU Proteomics Core with help and guidance of Lene H. Blicher and Assoc. Prof. Erwin M. Schoof.

Funding

The work is supported by the Novo Nordisk Foundation (NNF), Denmark Biotechnology Synthesis and Production (grant NNFOC0027616) and a third of a PhD stipend (to MM) from the Technical University of Denmark.

Appendix A. Supplementary data

Supplementary data to this article can be found online at https://doi.org/10.1016/j.fochms.2022.100137.

References

Abbate, R. A., Raak, N., Boye, S., Janke, A., Rohm, H., Jaros, D., & Lederer, A. (2019). Asymmetric flow field flow fractionation for the investigation of caseins cross-linked by microbial transglutaminase. *Food Hydrocolloids, 92*(1), 117–124. https://doi.org/10.1016/j.foodhyd.2019.01.043

Agyare, K. K., & Damodaran, S. (2010). pH-stability and thermal properties of microbial transglutaminase-treated whey protein isolate. *Journal of Agricultural and Food Chemistry, 58*(3), 1946–1953. https://doi.org/10.1021/jf903530d

Albani, J. R., Vogelaer, J., Bretesche, L., & Kmiecik, D. (2014). Tryptophan 19 residue is the origin of bovine β-lactoglobulin fluorescence. *Journal of Pharmaceutical and Biomedical Analysis, 91*, 144–150. https://doi.org/10.1016/j.jpba.2013.12.015

Chambers, M. C., MacLean, B., Burke, R., Amodei, D., Ruderman, D. L., Neumann, S., … Mallick, P. (2012). A cross-platform toolkit for mass spectrometry and proteomics. *Nature Biotechnology, 30*(10), 918–920. https://doi.org/10.1038/nbt.2377

Collini, M., D'Alfonso, L., & Baldini, G. (2000). New insight on β-lactoglobulin binding sites by 1-anilinonaphthalene-8-sulfonate fluorescence decay. *Protein Science, 9*(10), 1968–1974. https://doi.org/10.1110/ps.9.10.1968

Eissa, A. S., Puhl, C., Kadla, J. F., & Khan, S. A. (2006). Enzymatic cross-linking of β-lactoglobulin: Conformational properties using FTIR spectroscopy. *Biomacromolecules, 7*(6), 1707–1713. https://doi.org/10.1021/bm050928p

Færgemand, M., Otte, J., & Qvist, K. B. (1997). Enzymatic cross-linking of whey proteins by a Ca^{2+}-independent microbial transglutaminase from *Streptomyces lydicus*. *Food Hydrocolloids, 11*(1), 19–25. https://doi.org/10.1016/s0268-005x(97)80006-9

Gasteiger, E., Hoogland, C., Gattiker, A., Duvaud, S., Wilkins, M. R., Appel, R. D., & Bairoch, A. (2005). Protein identification and analysis tools on the ExPASy server. In *The Proteomics Protocols Handbook* (pp. 571–607). Humana Press. https://doi.org/10.1385/1-59259-890-0:571.

Gorji, E. G., Waheed, A., Ludwig, R., Toca-Herrera, J. L., Schleining, G., & Gorji, S. G. (2018). Complex coacervation of milk proteins with sodium alginate. *Journal of Agricultural and Food Chemistry, 66*(12), 3210–3220. https://doi.org/10.1021/acs.jafc.7b03915

Grossmann, L., Wefers, D., Bunzel, M., Weiss, J., & Zeeb, B. (2017). Accessibility of transglutaminase to induce protein crosslinking in gelled food matrices - Influence of network structure. *LWT - Food Science and Technology, 75*, 271–278. https://doi.org/10.1016/j.lwt.2016.09.005

Hemung, B. O., Li-Chan, E. C. Y., & Yongsawatdigul, J. (2009). Identification of glutaminyl sites on β-lactoglobulin for threadfin bream liver and microbial transglutaminase activity by MALDI-TOF mass spectrometry. *Food Chemistry, 115*(1), 149–154. https://doi.org/10.1016/j.foodchem.2008.11.098

Klemmer, K. J., Waldner, L., Stone, A., Low, N. H., & Nickerson, M. T. (2012). Complex coacervation of pea protein isolate and alginate polysaccharides. *Food Chemistry, 130*(3), 710–715. https://doi.org/10.1016/j.foodchem.2011.07.114

Krämer, A. C., Torreggiani, A., & Davies, M. J. (2017). Effect of oxidation and protein unfolding on cross-linking of β-Lactoglobulin and α-Lactalbumin. *Journal of Agricultural and Food Chemistry, 65*(47), 10258–10269. https://doi.org/10.1021/acs.jafc.7b03839

Kristiansen, K. R., Otte, J., Ipsen, R., & Qvist, K. B. (1998). Large-scale preparation of β-lactoglobulin A and B by ultrafiltration and ion-exchange chromatography. *International Dairy Journal, 8*(2), 113–118. https://doi.org/10.1016/s0958-6946(98)00028-4

Kuo, H. H., Chan, C., Burrows, L. L., & Deber, C. M. (2007). Hydrophobic interactions in complexes of antimicrobial peptides with bacterial polysaccharides. *Chemical Biology and Drug Design, 69*(6), 405–412. https://doi.org/10.1111/j.1747-0285.2007.00518.x

Liu, Y., Wu, H. C., Bhokisham, N., Li, J., Hong, K. L., Quan, D. N., Tsao, C. Y., Bentley, W. E., & Payne, G. F. (2018). Biofabricating functional soft matter using protein engineering to enable enzymatic assembly. *Bioconjugate Chemistry, 29*(6), 1809–1822. https://doi.org/10.1021/acs.bioconjchem.8b00197

Madsen, M., Westh, P., Khan, S., Ipsen, R., Almdal, K., Aachmann, F. L., & Svensson, B. (2021). Impact of alginate mannuronic-guluronic acid contents and pH on protein binding capacity and complex size. *Biomacromolecules, 22*(2), 649–660. https://doi.org/10.1021/acs.biomac.0c01485

Mensi, A., Choiset, Y., Rabesona, H., Haertlé, T., Borel, P., & Chobert, J. M. (2013). Interactions of β-lactoglobulin variants A and B with vitamin A. Competitive binding of retinoids and carotenoids. *Journal of Agricultural and Food Chemistry, 61*(17), 4114–4119. https://doi.org/10.1021/jf400711d

Merkley, E. D., Rysavy, S., Kahraman, A., Hafen, R. P., Daggett, V., & Adkins, J. N. (2014). Distance restraints from crosslinking mass spectrometry: Mining a molecular dynamics simulation database to evaluate lysine-lysine distances. *Protein Science, 23*(6), 747–759. https://doi.org/10.1002/pro.2458

Miwa, N. (2020). Innovation in the food industry using microbial transglutaminase: Keys to success and future prospects. *Analytical Biochemistry*, *597*(November 2019), 113638. https://doi.org/10.1016/j.ab.2020.113638.

Mostafa, H. S. (2020). Microbial transglutaminase: An overview of recent applications in food and packaging. *Biocatalysis and Biotransformation, 38*(3), 161–177. https://doi.org/10.1080/10242422.2020.1720660

Murphy, R. W., Farkas, B. E., & Jones, O. G. (2017). Effect of crosslinking on the physical and chemical properties of β-lactoglobulin (Blg) microgels. *Journal of Colloid and Interface Science, 505*, 736–744. https://doi.org/10.1016/j.jcis.2017.06.061

Nieuwenhuizen, W. F., Dekker, H. L., Gröneveld, T., De Koster, C. G., & De Jong, G. A. H. (2004). Transglutaminase-mediated modification of glutamine and lysine residues in native bovine β-Lactoglobulin. *Biotechnology and Bioengineering, 85*(3), 248–258. https://doi.org/10.1002/bit.10898

Partanen, R., Torkkeli, M., Hellman, M., Permi, P., Serimaa, R., Buchert, J., & Mattinen, M. L. (2011). Loosening of globular structure under alkaline pH affects accessibility of β-lactoglobulin to tyrosinase-induced oxidation and subsequent cross-linking. *Enzyme and Microbial Technology, 49*(2), 131–138. https://doi.org/10.1016/j.enzmictec.2011.04.010

Partschefeld, C., Richter, S., Schwarzenbolz, U., & Henle, T. (2007). Modification of β-lactoglobulin by microbial transglutaminase under high hydrostatic pressure: Localization of reactive glutamine residues. *Biotechnology Journal, 2*(4), 462–468. https://doi.org/10.1002/biot.200600226

Qi, L., Xu, Z., Jiang, X., Hu, C., & Zou, X. (2004). Preparation and antibacterial activity of chitosan nanoparticles. *Carbohydrate Research, 339*(16), 2693–2700. https://doi.org/10.1016/j.carres.2004.09.007

Raak, N., Abbate, R. A., Lederer, A., Rohm, H., & Jaros, D. (2018). Size separation techniques for the characterisation of cross-linked casein: A review of methods and their applications. In *Separations* (Vol. 5, Issue 1). https://doi.org/10.3390/separations5010014.

Roth-Walter, F., Afify, S. M., Pacios, L. F., Blokhuis, B. R., Redegeld, F., Regner, A., Petje, L. M., Fiocchi, A., Untersmayr, E., Dvorak, Z., Hufnagl, K., Pali-Schöll, I., & Jensen-Jarolim, E. (2021). Cow's milk protein β-lactoglobulin confers resilience against allergy by targeting complexed iron into immune cells. *Journal of Allergy and Clinical Immunology, 147*(1), 321–334.e4. https://doi.org/10.1016/j.jaci.2020.05.023

Schiener, P., Black, K. D., Stanley, M. S., & Green, D. H. (2015). The seasonal variation in the chemical composition of the kelp species *Laminaria digitata*, *Laminaria hyperborea*, *Saccharina latissima* and *Alaria esculenta*. *Journal of Applied Phycology, 27*(1), 363–373. https://doi.org/10.1007/s10811-014-0327-1

Schönbeck, C., Holm, R., Westh, P., & Peters, G. H. (2014). Extending the hydrophobic cavity of β-cyclodextrin results in more negative heat capacity changes but reduced binding affinities. *Journal of Inclusion Phenomena and Macrocyclic Chemistry, 78*(1–4), 351–361. https://doi.org/10.1007/s10847-013-0305-2

Seebacher, J., Mallick, P., Zhang, N., Eddes, J. S., Aebersold, R., & Gelb, M. H. (2006). Protein cross-linking analysis using mass spectrometry, isotope-coded cross-linkers, and integrated computational data processing. *Journal of Proteome Research, 5*(9), 2270–2282. https://doi.org/10.1021/pr060154z

Söderberg, C. A. G., Månsson, C., Bernfur, K., Rutsdottir, G., Härmark, J., Rajan, S., Al-Karadaghi, S., Rasmussen, M., Höjrup, P., Hebert, H., & Emanuelsson, C. (2018). Structural modelling of the DNAJB6 oligomeric chaperone shows a peptide-binding cleft lined with conserved S/T-residues at the dimer interface. *Scientific Reports, 8*(1), 1–15. https://doi.org/10.1038/s41598-018-23035-9

Søndergaard, M. T., Sorensen, A. B., Skov, L. L., Kjaer-Sorensen, K., Bauer, M. C., Nyegaard, M., Linse, S., Oxvig, C., & Overgaard, M. T. (2015). Calmodulin mutations causing catecholaminergic polymorphic ventricular tachycardia confer opposing functional and biophysical molecular changes. *FEBS Journal, 282*(4), 803–816. https://doi.org/10.1111/febs.13184

Stender, E. G. P., Khan, S., Ipsen, R., Madsen, F., Hägglund, P., Abou Hachem, M., Almdal, K., Westh, P., & Svensson, B. (2018). Effect of alginate size, mannuronic/guluronic acid content and pH on particle size, thermodynamics and composition of complexes with β-lactoglobulin. *Food Hydrocolloids, 75*, 157–163. https://doi.org/10.1016/j.foodhyd.2017.09.001

Stender, E. G. P., Koutina, G., Almdal, K., Hassenkam, T., Mackie, A., Ipsen, R., & Svensson, B. (2018). Isoenergic modification of whey protein structure by denaturation and crosslinking using transglutaminase. *Food and Function, 9*(2), 797–805. https://doi.org/10.1039/c7fo01451a

Tang, C.-H., & Ma, C.-Y. (2007). Modulation of the thermal stability of β-lactoglobulin by transglutaminase treatment. *European Food Research and Technology, 225*(5–6), 649–652. https://doi.org/10.1007/s00217-006-0460-4

Taulier, N., & Chalikian, T. V. (2001). Characterization of pH-induced transitions of β-lactoglobulin: Ultrasonic, densimetric, and spectroscopic studies. *Journal of Molecular Biology, 314*(4), 873–889. https://doi.org/10.1006/jmbi.2001.5188

Tavares, G. M., Croguennec, T., Hamon, P., Carvalho, A. F., & Bouhallab, S. (2015). Selective coacervation between lactoferrin and the two isoforms of β-lactoglobulin. *Food Hydrocolloids, 48*, 238–247. https://doi.org/10.1016/j.foodhyd.2015.02.027

Tokai, S., Uraji, M., & Hatanaka, T. (2020). Molecular insights into the mechanism of substrate recognition of Streptomyces transglutaminases. *Bioscience, Biotechnology and Biochemistry, 84*(3), 575–582. https://doi.org/10.1080/09168451.2019.1697198

Wichchukit, S., Oztop, M. H., McCarthy, M. J., & McCarthy, K. L. (2013). Whey protein/alginate beads as carriers of a bioactive component. *Food Hydrocolloids, 33*(1), 66–73. https://doi.org/10.1016/j.foodhyd.2013.02.013

Yousefi, M., & Jafari, S. M. (2019). Recent advances in application of different hydrocolloids in dairy products to improve their techno-functional properties. *Trends in Food Science and Technology, 88*(April), 468–483. https://doi.org/10.1016/j.tifs.2019.04.015